



Monitoring the Atlantic meridional overturning circulation

Darren Rayner^{a,*}, Joël J.-M. Hirschi^a, Torsten Kanzow^b, William E. Johns^c, Paul G. Wright^a, Eleanor Frajka-Williams^a, Harry L. Bryden^a, Christopher S. Meinen^d, Molly O. Baringer^d, Jochem Marotzke^e, Lisa M. Beal^c, Stuart A. Cunningham^a

^a Ocean Observing and Climate Research Group, National Oceanography Centre, Southampton, United Kingdom

^b Ozeanzirkulation und Klimadynamik, Leibniz-Institut für Meereswissenschaften an der Universität Kiel, Kiel, Germany

^c Division of Meteorology and Physical Oceanography, Rosenstiel School of Marine and Atmospheric Science, Miami, FL, USA

^d Physical Oceanography Division, National Oceanic and Atmospheric Administration, Atlantic Oceanographic and Meteorological Laboratory, Miami, FL, USA

^e Max-Planck-Institut für Meteorologie, Hamburg, Germany

ARTICLE INFO

Article history:

Received 12 October 2010

Accepted 12 October 2010

Available online 27 January 2011

Keywords:

Physical oceanography

Thermohaline circulation

Ocean circulation

Ocean currents

Mooring systems

Atlantic meridional overturning circulation

ABSTRACT

The rapid climate change programme (RAPID) has established a prototype system to continuously observe the strength and structure of the Atlantic meridional overturning circulation (MOC) at 26.5°N. Here we provide a detailed description of the RAPID-MOC monitoring array and how it has evolved during the first four deployment years, as well as an overview of the main findings so far. The RAPID-MOC monitoring array measures: (1) Gulf Stream transport through Florida Strait by cable and repeat direct velocity measurements; (2) Ekman transports by satellite scatterometer measurements; (3) Deep Western Boundary Currents by direct velocity measurements; (4) the basin wide interior baroclinic circulation from moorings measuring vertical profiles of density at the boundaries and on either side of the Mid-Atlantic Ridge; and (5) barotropic fluctuations using bottom pressure recorders. The array became operational in late March 2004 and is expected to continue until at least 2014. The first 4 years of observations (April 2004–April 2008) have provided an unprecedented insight into the MOC structure and variability. We show that the zonally integrated meridional flow tends to conserve mass, with the fluctuations of the different transport components largely compensating at periods longer than 10 days. We take this as experimental confirmation of the monitoring strategy, which was initially tested in numerical models. The MOC at 26.5°N is characterised by a large variability—even on timescales as short as weeks to months. The mean maximum MOC transport for the first 4 years of observations is 18.7 Sv with a standard deviation of 4.8 Sv. The mechanisms causing the MOC variability are not yet fully understood. Part of the observed MOC variability consists of a seasonal cycle, which can be linked to the seasonal variability of the wind stress curl close to the African coast. Close to the western boundary, fluctuations in the Gulf Stream and in the North Atlantic Deep Water (NADW) coincide with bottom pressure variations at the western margin, thus suggesting a barotropic compensation. Ongoing and future research will put these local transport variations into a wider spatial and climatic context.

© 2011 Elsevier Ltd. All rights reserved.

1. Introduction

Large variations in the Earth's climate have occurred in the past according to paleo records. Some of the variations during the last 100,000 years were rapid, with 10 °C changes in Greenland temperature occurring over a period of 5–25 years (Broecker and Denton, 1989; Dansgaard et al., 1993; Huber et al., 2006). These rapid changes are generally attributed to changes in the strength of the Atlantic meridional overturning circulation (MOC). The

Atlantic MOC carries warm upper waters northward through the Atlantic; the waters gradually cool on their journey northward giving up heat to the atmosphere; in the subpolar and polar regions the surface waters become cold and salty enough to sink to the bottom forming cold deep waters; and this cold deep water returns southward through the Atlantic (Ganachaud and Wunsch, 2002). The magnitude of the Atlantic MOC is estimated to be about 17 Sv and it transports 1.3 PW of heat northward, an amount equal to a quarter of the maximum poleward heat transport of the combined global atmosphere–ocean heat transport required to balance the global heat budget (Bryden and Imawaki, 2001). It is generally thought that switching off this MOC – e.g. as hypothesised to be caused by the melting of ice caps

* Corresponding author.

E-mail address: dr400@noc.soton.ac.uk (D. Rayner).

in the early warming period at the end of the ice age – would lead to the rapid cooling of the northern Atlantic, and switching on the MOC would lead to the rapid warming found in paleo records.

The Earth's climate has been remarkably stable for the past 8000 years and this stable climate has coincided with, and arguably contributed to, the development of modern civilisation from prehistoric nomadic tribes to modern industrial society. We are now performing a finite amplitude perturbation experiment on the climate system by doubling the amount of CO₂ in the atmosphere. Will we perturb the climate out of its stable state? Because of its role in past rapid climate change events, the Atlantic meridional overturning circulation is a focus for understanding present and future climate changes.

Coupled ocean-atmosphere climate models are in agreement that the Atlantic MOC will decrease as CO₂ builds up in the atmosphere (Cubasch et al., 2001; IPCC, 2007). Eleven coupled models run under greenhouse gas forcing where CO₂ doubles every 70 years, all show a decrease in the Atlantic MOC by 10–50% over 140 years (Gregory et al., 2005). The slowdown in the MOC is gradual, however, no model exhibits a sudden change in the overturning circulation. On the other hand, experiments with coupled models using a fixed CO₂ level, where deep water formation is turned off by adding freshwater to the surface waters of the northern Atlantic, exhibit a rapid shutdown of the MOC resulting in 4–8 °C reductions in air temperatures over the northern Atlantic and northwest Europe (Vellinga and Wood, 2002). Thus, our best models predict a weakening of the Atlantic MOC under an increase in CO₂ in the atmosphere and suggest that if the MOC abruptly shuts down there would be severe cooling over the northern Atlantic.

There is confusion about how the North Atlantic circulation is changing. Some ocean observations suggest a slowdown of the MOC by as much as 30% over the last 50 years with the change in structure so that less North Atlantic Deep Water flows southward, and more upper waters are circulated in the subtropical gyre (Bryden et al., 2005). A possible weakening of the MOC is supported by observations of a cessation in the formation of lower North Atlantic Deep Water (Østerhus and Gammelsrod, 1999), a decrease in the amount of cold dense overflow waters through the Faroe Bank Channel (Hansen et al., 2001), reduced northward flow of upper waters through the subpolar gyre (Lherminier et al., 2006), and a freshening of northern Atlantic surface and deep waters (Curry et al., 2003; Dickson et al., 2002). However other observations do not support a weakening MOC. Olsen et al. (2008) found that there was no trend in the Faroe Bank Channel overflow, and Holliday et al. (2008) report a reversal of the previously observed freshening trend of the northeast North Atlantic and Nordic Seas—possibly caused by a reduced contribution of water from the subpolar gyre (Hátún et al., 2005; Häkkinen and Rhines, 2004) or by surface waters from the Gulf Stream reaching the Rockall Trough through the subtropical gyre (Häkkinen and Rhines, 2009). For more discussion on the evidence for the changing MOC, see Cunningham and Marsh (2010).

North Atlantic surface temperatures are increasing, even faster than temperatures in the North Pacific, for example. How can we reconcile warmer sea surface temperatures with a slowdown in the MOC? Analyses of natural variability in coupled climate models run over 1000-year periods indicate that warmer Atlantic temperatures are significantly correlated with a stronger MOC. Warmer Atlantic sea surface temperatures (SSTs) could be a direct result of radiative heating due to the greenhouse effect associated with increased CO₂ in the atmosphere (Cubasch et al., 2001; IPCC, 2007). However, warmer SSTs could also be associated with high North Atlantic Oscillation (NAO) and Atlantic Multidecadal Oscillation (AMO) indices. The NAO index measures the strength of the

westerly winds over the northern Atlantic. This index has increased substantially from the 1970s to the 1990s and the low frequency response to sustained NAO forcing is expected to be warmer SSTs (Visbeck et al., 2003). The AMO is a natural oscillation of 50–100-year period in the Atlantic, which combines a strong MOC and warm SSTs (Delworth and Mann, 2000). The warmer SSTs in the past 25 years are then taken as evidence that the Atlantic MOC is presently in a strong phase (Knight et al., 2005). For comparison, the 11 coupled climate model runs with doubling atmospheric CO₂ over 70 years all show slowing of the Atlantic MOC but an overall warming of Atlantic temperature; the cooling associated with a gradual decrease of the MOC is smaller than the warming associated with direct radiative forcing, so everywhere in the Atlantic SSTs increase with time (Gregory et al., 2005). Thus, there are many views on the reason for an increase in SSTs in the North Atlantic, but it is possible that a cooling trend associated with a slowdown in the Atlantic MOC is being masked by direct radiative heating due to increased atmospheric CO₂. However, even in this case, it is not yet understood why the North Atlantic region warms faster than, e.g. the North Pacific.

There is a clear need for observations of the Atlantic MOC and how it is changing over time. The MOC is central to our understanding of the present climate and how it might change in the future. Thus, it is essential to establish a baseline measure of the MOC strength and its seasonal to interannual variability to put wide-ranging and longer timeseries of Atlantic observations into an overall context of Atlantic (and global) climate change. Comparison of a timeseries of the observed strength of the MOC with SSTs, NAO index and AMO index would clarify the relationship between presently distinct phenomena. Finally, we want to know if there is a trend in the strength of the MOC and whether it is a significant decrease (or increase) in the overturning circulation.

In this paper we describe an array deployed at 26.5°N to continuously monitor the MOC, with a description of the observational strategy and the pre-deployment design validation with numerical models (Section 2). The array has evolved over time and these changes are summarised in Section 2.5. A summary of the main scientific findings is given in Section 3 and in Section 4 we provide a discussion of these results and place them in the wider context of measuring the MOC.

2. Monitoring programme

We initiated a monitoring project in 2004 with timeseries measurements of the basin-scale overturning circulation at 26.5°N (Fig. 1) (Marotzke et al., 2002). The project was funded from 2004 to 2008 in the framework of the Rapid Climate Change (RAPID) thematic programme of the Natural Environment Research Council (NERC), the National Science Foundation (NSF) Meridional Circulation and Heat Flux Array (MOCHA) and by the NOAA Office of Climate Observations. Funding has since been extended by NERC, NSF and NOAA till 2014 as part of the RAPID-WATCH (Will the Atlantic Thermohaline Circulation Halt?) programme to provide a decade long timeseries of measurements. The main aim of the project is the development of an operational, cost-efficient observation system that continuously monitors the strength and vertical structure of the Atlantic MOC at 26.5°N.

2.1. Rationale for observing the MOC at 26.5°N

The latitude of 26.5°N for the monitoring array was chosen for three reasons: it is close to the peak northward heat transport; it is the latitude of four modern hydrographic sections (five including one in 2004 immediately after the array was deployed);

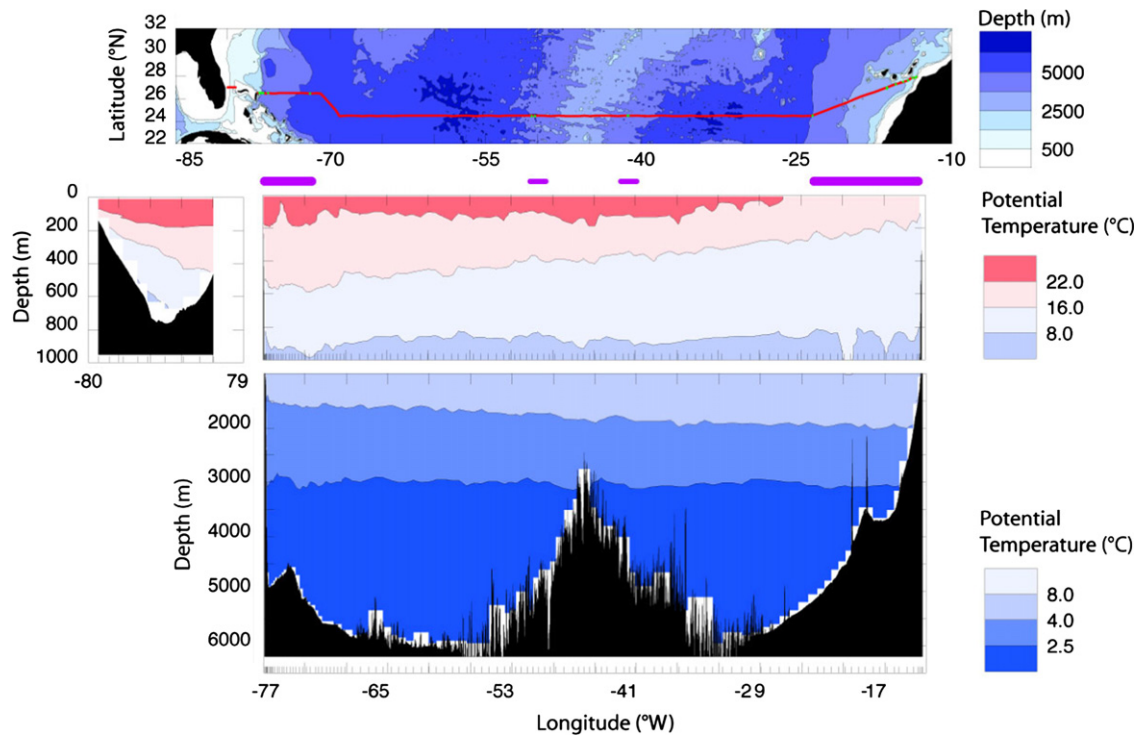


Fig. 1. Top panel: Bathymetry of the North Atlantic subtropical gyre region. The red line from Bahamas to Africa represents the track of the 2004 hydrographic section (Cunningham, 2005b) whose temperature distribution is shown in the three panels below. The middle left hand panel shows the temperature distribution of the northward flowing Gulf Stream in the Florida Strait. The middle panel shows the temperature distribution of the upper 1000 m—the isotherms sloping up to the east are indicative of the southward flow of thermocline water. The lower panel shows the temperature distribution of the lower 5000 m of the water column, which is generally moving southward. Magenta bars below the top panel denote the regions of the RAPID moorings sub-arrays. (For interpretation of the references to color in this figure legend, the reader is referred to the web version of this article.)

the western boundary current (flow through the Florida Strait) has a long history of measurements and can be measured relatively straightforwardly by cable and regular calibration cruises (Larsen, 1992, Baringer and Larsen, 2001). Additionally, 26.5°N has the advantage of having comparatively steep basin boundaries compared to other latitudes.

2.2. Observational strategy

The Atlantic MOC is decomposed into three components that can be measured separately: (1) The Gulf Stream transport T_{GS} through the Florida Straits (Baringer and Larsen, 2001), (2) the near-surface wind driven Ekman component T_{EK} and (3) the mid-ocean flow T_{MO} between the Bahamas and Africa (Fig. 2).

At 26.5°N the Gulf Stream flows through the narrow (80 km), shallow (800 m) Florida Straits between Florida and the Bahamas. The Gulf Stream transport has been estimated for more than 25 years by recording the induced voltage on submerged telephone cables between West Palm Beach and Grand Bahama Island (Baringer and Larsen, 2001). A conductor (in this case seawater) passing through the Earth's magnetic field will induce an electric field perpendicular to the motion of the conductor. This induced electric field varies in relation to the rate of flow of the conductor and can be detected by voltage changes on the telephone cable relative to an Earth ground. The voltage variations are calibrated with direct estimates of the Gulf Stream transport from the velocity profiles from Lowered Acoustic Doppler Current Profiler (LADCP) sections and mean vertical current profiles collected by Dropsonde floats (Larsen, 1992) to give T_{GS} . Daily mean transport estimates are used in the calculation of the MOC.

T_{EK} is derived from satellite based measurements of the wind stress, and is integrated from west to east across the Atlantic

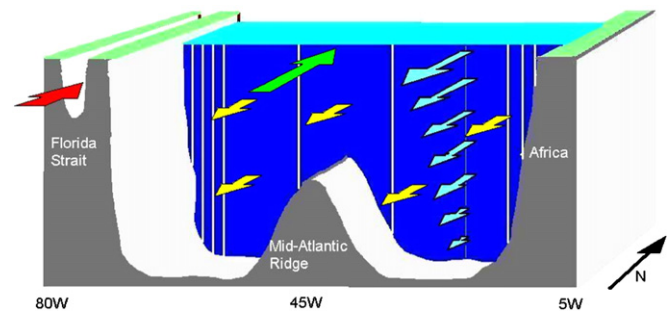


Fig. 2. Schematic of the MOC monitoring array at 26°N. The MOC is decomposed into three components: (1) Gulf Stream transport T_{GS} through the Florida Straits (red arrow), (2) the near-surface wind driven Ekman transport T_{EK} (green arrow) arising from the zonal wind stress and (3) geostrophic (thermal wind) contribution T_{INT} (light blue arrows) calculated between adjacent pairs of "moorings" (vertical lines). Yellow arrows indicate a spatially constant velocity correction that ensures mass balance across the section. (For interpretation of the references to color in this figure legend, the reader is referred to the web version of this article.)

according to

$$T_{EK} = - \int \frac{\tau_x}{\rho f} dx$$

where τ_x is the zonal component of the wind stress, ρ is water density and f the Coriolis parameter. τ_x is inferred from Quick SCAT scatterometer measurements of the roughness of the sea surface (Graf et al., 1998). Wind stress estimates are available at a daily resolution. Kanzow et al. (2010) estimate the possible 4-year mean bias in T_{EK} to be ± 0.5 Sv.

We decompose T_{MO} into three components that are observed by a trans-Atlantic array of moorings between the Bahamas and the coast of Africa. T_{INT} is the internal geostrophic flow, T_{EXT} is the

zonally integrated reference-level contribution of the geostrophic flow and T_{WBW} is the meridional transport over the continental shelf west of the moorings WB1 and WB2—referred to as the western boundary wedge.

T_{INT} is calculated from the difference in full depth density profiles on either side of the Atlantic basin with the profiles derived from temperature, conductivity and pressure measurements at discrete levels—hereafter referred to as geostrophic moorings. In the west the continental shelf slope is steep and the tall geostrophic mooring WB2 is placed close to the Bahamas escarpment. In the east the shelf slope is much more gradual so a series of shorter moorings is distributed up the slope to minimise the effects of bottom triangles where horizontal interpolation at depth would miss significant sections of the ocean (e.g. Whitworth and Peterson, 1985). This series of moorings is merged to produce a single vertical density profile at the eastern boundary. The eastern and western density profiles give the geostrophic internal transport (T_{INT}) relative to the reference level (Z_{REF}) using

$$T_{INT}(z) = -g/(f\rho) \int_{Z_{REF}}^0 [\rho_E(z') - \rho_W(z')] dz$$

where g is the Earth's acceleration of gravity, ρ_E the density in the east and ρ_W the density in the west. We use a reference level of -4740 m.

Bottom pressure recorders are used to compute the time-varying reference level meridional geostrophic velocities. From these the vertically integrated external transport fluctuation (T_{EXT}^i) integrated between two sites i and $i+1$ can be obtained using

$$T_{EXT}^i = H^i/(f\rho)[P_{BOT}^{i+1} - P_{BOT}^i]$$

where H is the water column height and P_{BOT} is the bottom pressure at each site. As H is different for each site the deeper of the two is adjusted to the shallower one by removing the density fluctuations below the depth of the shallower site found from the geostrophic mooring nearest to the deeper site. The zonal transport integral T_{EXT} is found by summing the contributions between adjacent moorings so that

$$T_{EXT} = \sum T_{EXT}^i$$

The western boundary wedge component (T_{WBW}) is obtained from interpolating and integrating direct velocity measurements from current metres on moorings inshore of the westernmost density mooring (Johns et al., 2007). Currents in this region consist of the upper-ocean northward Antilles current and the upper and inshore fractions of the Deep Western Boundary Current (DWBC).

If we assume there is no net mass transport across 26.5°N then we can simplify this with the vertical integral of T_{MO} equalling the vertical integral of the sum of T_{EK} and T_{GS} . This method does not use T_{EXT} and instead adds a barotropic transport profile to T_{INT} to maintain mass balance at each time step. Kanzow et al. (2007) show the validity of this approach.

The timeseries of the MOC—defined as the maximum northward upper-ocean transport is produced by summing T_{GS} , T_{EK} and T_{UMO} transports, where T_{UMO} is the upper mid-ocean transport found by vertically integrating T_{MO} down to the deepest northward velocity (~ 1100 m) on each day.

2.3. Array design tests in numerical models

Numerical ocean models are a valuable tool for testing the *ad hoc* observational strategy. Prior to the deployment of the RAPID-MOC array we have used models to compare the MOC calculated from the full meridional velocities to reconstructions based on

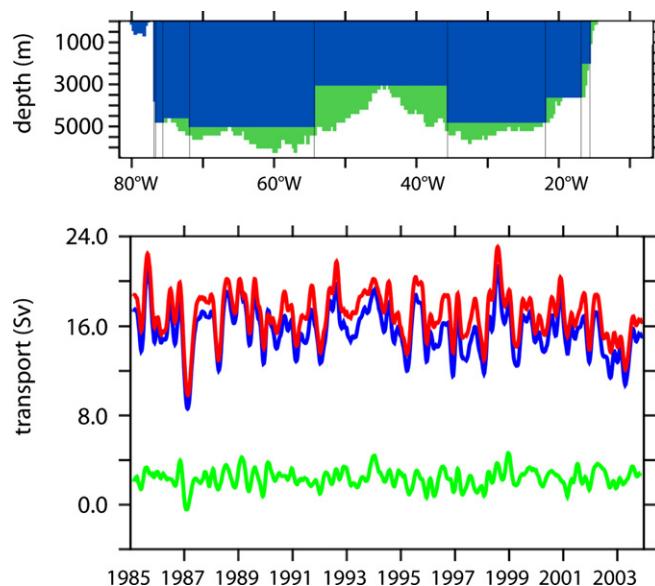


Fig. 3. Testing the MOC monitoring strategy in an eddy-permitting ocean model (OCCAM; Webb 1996). The horizontal resolution is 0.25° in both longitude and latitude. Top: placement of “moorings” (vertical lines) and area where velocity can be calculated based on zonal density differences (blue area). Bottom: MOC at 26.5°N and 1100 m depth (blue), reconstruction (red, see main text) and Ekman contribution (green). (For interpretation of the references to color in this figure legend, the reader is referred to the web version of this article.)

sub-sampled model data (Hirschi et al., 2003, Baehr et al., 2004, Hirschi and Marotzke, 2007). We obtain the reconstructions by summing the modelled transport through the Florida Straits, the Ekman transport calculated from the zonal wind stress used to force the model at the surface and the geostrophic transport obtained from “moorings” deployed in the numerical model. Additionally, we add a spatially constant velocity correction so that there is no net mass transport across the longitude-depth section at 26.5°N (Fig. 2). The high level of agreement found between the simulated MOC and its estimate based on the proposed observing strategy provides a first indication for the soundness of the approach (Fig. 3) (Hirschi et al., 2003, Baehr et al., 2004, Hirschi and Marotzke, 2007).

2.4. Implementation and deployment of the array

The mooring array consists of three sub-arrays: one at the western boundary (east of the Bahamas), one at the eastern boundary (west of Morocco) and one with moorings on either side of the Mid-Atlantic Ridge. The western boundary and eastern boundary moorings provide endpoint density profiles used during the calculation of the ocean-wide zonally integrated geostrophic flow. The Mid-Atlantic Ridge moorings allow the contribution to the MOC from the eastern and western basins to be distinguished.

A mooring to obtain a vertical density profile timeseries comprises a series of self-logging conductivity, temperature and depth instruments (CTDs) vertically distributed on an anchored mooring wire supported by distributed buoyancy. Vertical instrument resolution increases at shallower depths where the higher vertical density gradient requires more reference points for an accurate interpolation of the density profile. The instruments are typically set to record data at 15–30 min intervals with data subsequently low-pass-filtered to remove tides. Moorings are serviced annually with the western boundary serviced in Spring and the eastern boundary and Mid-Atlantic Ridge sub-arrays serviced in Autumn.

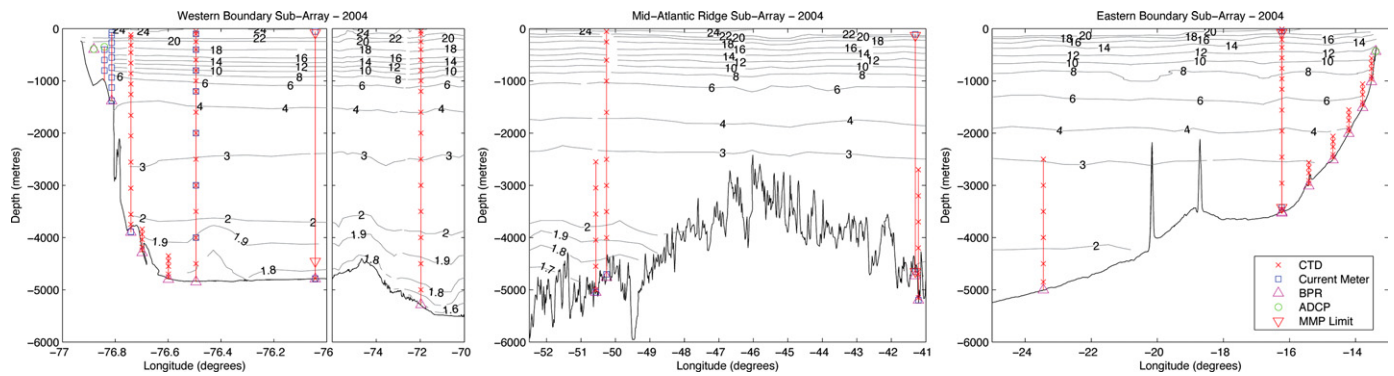


Fig. 4. Schematic of the three RAPID mooring sub-arrays as deployed in March and April 2004 (Cunningham, 2005a). Moorings are the vertical red lines and instrument symbols are defined in the key on the right hand panel (CTD—conductivity, temperature, depth recorder; current meter—direct velocity measuring instrument; BPR—bottom pressure recorder measuring the hydrostatic weight of water, ADCP—an acoustic Doppler current profiler and MMP limit is the profiling range of a profiling self propelled CTD). Distribution of potential temperature was obtained on a trans-Atlantic hydrographic transect in 2004 following the deployment of the mooring arrays (Cunningham, 2005b). (For interpretation of the references to color in this figure legend, the reader is referred to the web version of this article.)

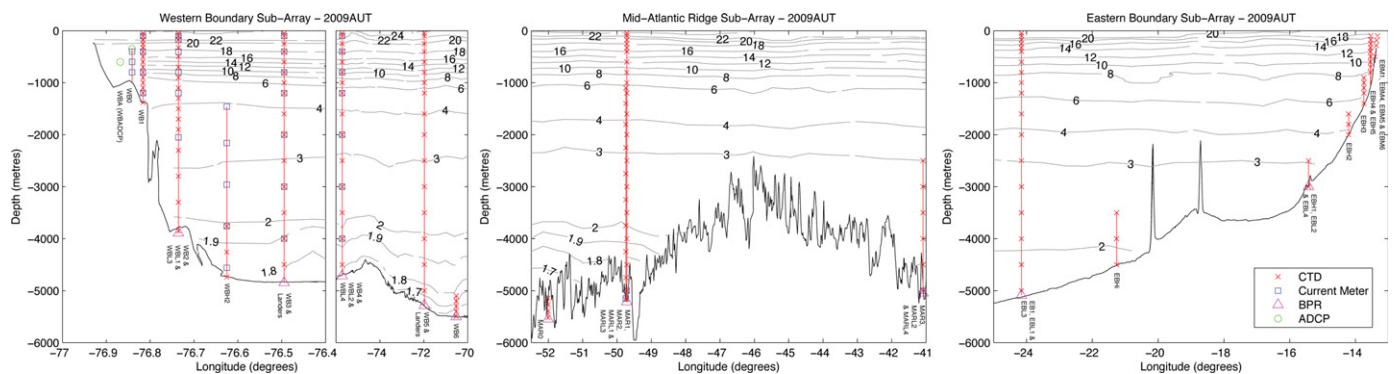


Fig. 5. As Fig. 4 but for mooring deployments from 2009 to 2010.

The western boundary sub-array is the most important: the largest fluctuations in the Atlantic MOC occur here compared to the rest of the ocean basin. Our key mooring WB2, measuring between 50 and 3800 m depth, is deployed as close as possible (< 3 km) to the “wall” of the continental shelf. WB3 (50–4800 m; 27 km offshore from WB2) and WB1 (50–1400 m; 7 km inshore from WB2) can be used as backups to provide the density profile if WB2 is lost. WB1, WB0 and WBA also use current meters to directly measure the DWBC and the shallower Antilles current, allowing the flow inshore of the geostrophic array to be measured. WB4 and WB5 are deployed offshore from the principal moorings to monitor the offshore extent of the DWBC, thus capturing thermal wind shear across the entire boundary current.

In the east, to minimise leakage through bottom triangles, a series of shorter moorings (EBH1–EBH5) were deployed up the slope. As the array evolved this series was extended with EBHi at the deeper end and a series of still smaller “mini-moorings”, EBM1–EBM7, added at the inshore end to reduce risk of data loss through fishing activity.

The series of moorings in the east is merged to create a single profile as the counterpart to WB2. This is a change from our initial strategy where we had the tall mooring EB2 deployed in deep water—with its location chosen as a compromise between the desire for full water depth and the nearness to the shelf break.

The contribution to MOC variability from the eastern and western basins can be distinguished by the Mid-Atlantic Ridge moorings. MAR1 (up to 50 m depth) and MAR2 (up to 1100 m) are deployed on the western flank of the ridge, with MAR3 (up to the ridge crest at 2500 m) and MAR4 (up to 50 m) initially deployed on the eastern flank.

2.5. Evolution of the mooring array

The array as first deployed in 2004 consisted of 22 moorings (Fig. 4) with the primary geostrophic moorings being WB2 in the west and EB2 in the east. EB3 was deployed 10 km from EB2 as a backup. The backup to WB2 was WB3, 24 km further offshore. The vertical resolution of density measurements was 14 discrete levels at the 3900 m deep WB2 site and 13 discrete levels at the 3500 m deep EB2 site. The array configuration has been progressively modified during subsequent deployments, with the current configuration shown in Fig. 5.

WB2 is still our primary density mooring in the west but the instrument vertical resolution has been increased to 22 (when merging the upper 1400 m with WB1) to allow better interpolation of the density profile. At the eastern margin EB2 was relocated offshore to the site of EB1 in 5100 m depth following damage to the mooring during the first year's deployment—EB1 was extended to 50 m depth to act as the backup and EB3 was removed from the array. Subsequently the work by Kanzow et al. (2010) demonstrated the importance of the continental slope region for capturing seasonal variability in the MOC so the focus for the eastern boundary density profile is now the series of short moorings that steps up the slope. As such the EB2 site is less important and so the EB1 backup mooring is not required.

The series of shorter moorings has changed slightly as the array has evolved to try to minimise risk of loss through fishing activity on the continental slope. The current design has a series of mini-moorings (EBM1, 4, 5 and 6) at the inshore end, which each consist of a single instrument, thereby spreading the risk of losing all of the shallow data records. Experience has shown that

the Mid-Atlantic Ridge moorings are relatively safe so the number of geostrophic moorings deployed here has been reduced from four to three, with MAR4 being removed. The pressure gradient across the ridge is monitored by the moorings profiling up to the ridge crest, with MAR1 providing the upper water column profile for both sides of the ridge.

In the western boundary sub-array WBH1 and WBH2 were removed from the array with WBH2 subsequently being reinstated but with a different design to include current meters for better horizontal interpolation of direct velocity measurements of the Deep Western Boundary Current.

The bottom pressure recorders (BPRs) deployed in the first year were attached to drop off mechanisms to the bottom of the moorings by magnesium bolts. When these bolts corrode after a couple of hours the BPRs are dropped to the seabed to decouple them from mooring motion. The BPR remained attached to the mooring by a short length of rope so that when the main mooring was recovered the BPR was recovered too. Due to the large and somewhat unpredictable drift that pressure sensors can exhibit the 1-year timeseries is often not enough to remove the drift satisfactorily. The BPRs were removed from the moorings and deployed on their own custom moorings – termed landers – that mount the BPR on a stable frame on the seabed. These are now deployed for 2 years at a time with overlapping records of 1 year so that the second half of the record (which is less affected by drift) can be used for the calculations of T_{EXT} .

Another change that has taken place in the array design is the deployment of moorings MAR0 on the western flank of the Mid-Atlantic Ridge and WB6 640 km offshore of the Bahamas in the western boundary sub-array. These moorings are both at a depth of 5500 m and have been deployed to study the contribution to the MOC variability from Antarctic Bottom Water.

2.6. The use of gliders in the array

Two autonomous glider missions have been undertaken to assess the contribution that autonomous gliders could make in monitoring the MOC, with a specific focus on their use as a substitute for moorings at the eastern boundary. This part of the RAPID array has suffered losses of instruments and data—largely due to suspected fishing activity on the continental slope. Furthermore, the findings of Kanzow et al. (2010) mean that the data from this area are more important than the first thought. It is expected that gliders will be less susceptible to loss by fishing (in particular trawling) than the moored instruments and hence improve data return from this region. Another advantage of gliders is that data may be retrieved in real-time via iridium satellite communications, thus further reducing the risk of data loss.

These glider missions took place between 15 September–24 November 2008 and 21 May–21 July 2009, between the Canary Islands and the coast of Morocco. The findings are being prepared for a subsequent paper (Smeed et al., 2010).

3. Results

In the following we are summarizing the most important scientific findings of the first 4 years of continuous MOC observations at 26.5°N in the Atlantic.

Prior to RAPID the validity of the RAPID monitoring approach for the MOC was based on tests performed with numerical ocean models. One main assumption that was made is that the sum of T_{CS} , T_{EK} and T_{INT} is compensated by a zonally constant, barotropic flow across the section. The net (top to bottom integrated) meridional flow across 26.5°N should be small because there is

only a small (~ 1 Sv, $1 \text{ Sv} \equiv 10^6 \text{ m}^3 \text{ s}^{-1}$) net flow through the Atlantic due to Pacific to Atlantic flow through the Bering Strait and a net input of freshwater from the atmosphere, rivers and ice northward of 26.5°N. Thus, the different transport components we observe (Fig. 6A) should compensate for each other, such that an overall mass balance is achieved. Kanzow et al. (2007) demonstrate that this mass balance exists at periods longer than 10 days (Fig. 6B), with the sum of Gulf Stream and Ekman transports fluctuating in anti-phase with the geostrophic flow between the Bahamas and the African coast. Kanzow et al. (2007) interpret the compensation between T_{EXT} and T_{CS} , T_{EK} , T_{INT} as observational evidence that the monitoring approach taken is valid and that the RAPID system is working reliably since T_{EXT} is equivalent to the simple compensation assumed in our numerical tests.

Based on the above transport observations, a year-long time-series of the strength of the MOC was derived by Cunningham et al. (2007), defined as the maximum northward upper ocean transport for each day between April 2004 and March 2005. The flow is found to be northward between the sea surface and roughly the 1100 m depth level – as a consequence of the northward flow of the Gulf Stream, the Antilles Current and the Ekman flow – and is compensated by a southward flow below that, concentrated mostly within the Deep Western Boundary Current (Johns et al., 2007), a stream that flows along the continental slope of the Americas and exports the North Atlantic Deep Waters into the other ocean basins. A remarkable feature emerging from the first deployment year is the large variability found for the maximum MOC at 26.5°N—even on subannual timescales.

We have now extended the MOC timeseries to 4 years from 2 April 2004 to 10 April 2008. At 26.5°N the strength of the MOC (10-day low-pass filtered) (Fig. 7) has a mean of 18.7 Sv and varies by ± 4.8 Sv (one standard deviation) over the 4-year period

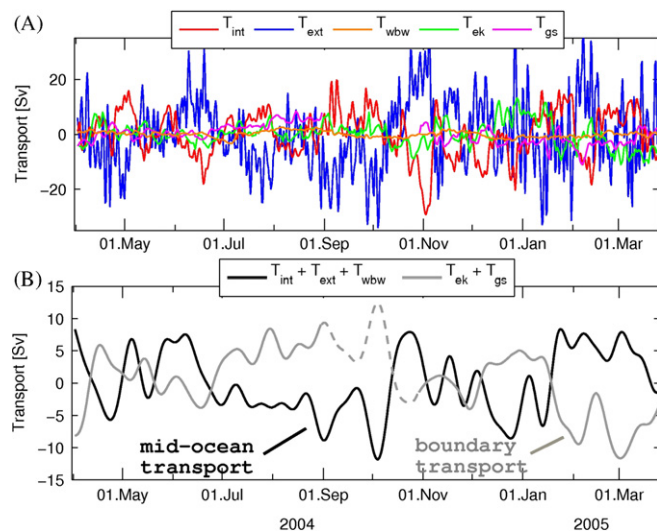


Fig. 6. Top panel: fluctuations of vertically integrated internal (T_{INT} , red), external (T_{EXT} , blue), western boundary wedge (T_{WBW} , orange), Ekman (T_{EK} , green) and Gulf Stream (T_{CS} , magenta) transports. The transport T_{EXT} is obtained from measurements of the bottom pressure and is equivalent to the depth-independent transport correction used in the numerical tests (see Fig. 2). There is a two-month gap in T_{CS} between 31/08/2004 and 29/09/2004. All timeseries have been 2-day low-pass filtered and sub-sampled on a half-daily grid. The initial sampling rates were 15 min for the underlying density and current measurements and 10 min for bottom pressure. Bottom panel: 15-day low-pass filtered fluctuations of vertically integrated mid-ocean ($T_{MO} = T_{INT} + T_{EXT} + T_{WBW}$) and boundary transports ($T_{BOUND} = T_{EK} + T_{CS}$) as black and grey lines, respectively. The dashed part of the grey line denotes the period when T_{CS} could not be measured. A linear regression between T_{MO} and T_{BOUND} is used to fill this gap (Kanzow et al., 2007). (For interpretation of the references to color in this figure legend, the reader is referred to the web version of this article.)

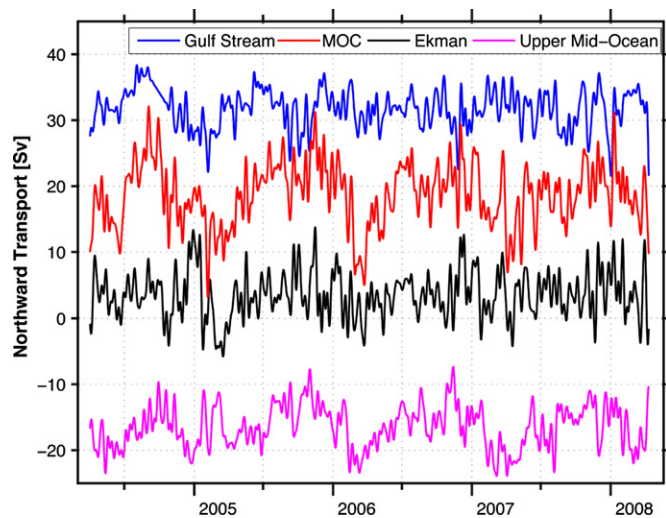


Fig. 7. Daily timeseries of Gulf Stream transport (blue), Ekman transport (black), upper mid-ocean transport (magenta) and overturning transport (red) for the period 2 April 2004–10 April 2008. Gulf Stream transport is based on electromagnetic cable measurements in the Florida Straits. A gap in the timeseries of approximately two months from 4 September to 28 October 2004 is due to Hurricane Frances, which destroyed the facility recording the voltage. Here linear interpolation is chosen to fill the gap. Ekman transport is based on QuikSCAT winds. The upper mid-ocean transport is based on the RAPID array measurements and is the vertical integral of the transport per unit depth down to the deepest northward velocity (~ 1100 m) on each day. Overturning transport is then the sum of the Gulf Stream, Ekman and upper mid-ocean transports and represents the maximum northward transport of upper layer waters on each day. (For interpretation of the references to color in this figure legend, the reader is referred to the web version of this article.)

of observations, occupying a range of values between 3.2 and 32.1 Sv. The MOC changes in strength on seasonal timescales but also at periods as short as weeks to months. All components (T_{GS} , T_{EK} and T_{UMO}) contribute about equally to the total MOC variability (Fig. 7). Whereas it was previously known that the Ekman and Gulf Stream transports can exhibit a large variability on subannual to interannual timescales, our observations were the first to show that a similar variability is found for the mid-ocean transport T_{UMO} .

The nature of the MOC variability (in particular the contributions from T_{UMO} and T_{GS}) observed at 26.5°N is far from fully understood. Possible sources of variability include internal waves (Rossby and Kelvin waves) and eddies. However, the imprint of waves and/or eddies on the MOC is difficult to quantify. Results from a numerical model suggest that transport anomalies tend to propagate westward with a velocity similar to that expected for Rossby waves or eddies (Hirschi et al., 2007). Both eddies and Rossby waves have a signature in the sea surface height. Therefore, if internal waves or eddies were the main cause of the observed variability in T_{UMO} , one would expect to find a significant correlation between T_{UMO} and the sea surface height (SSH) variability. Surprisingly, the rms sea surface height variability observed in both dynamic heights from in situ density measurements and altimetric heights reduces by a factor of three, approaching the western boundary over a distance of 100 km (Fig. 8). As a consequence of this suppression of variability right at the western boundary the variability of T_{UMO} is only 3.0 Sv rms. Correlations of the SSH and T_{UMO} are also small close to the western boundary. This lack of a relationship between surface height and upper ocean transport is related to an increase in importance of higher order vertical modes of horizontal velocity right at the western boundary. This deterioration of the SSH- T_{UMO} correlation is found in both the RAPID observations (Kanzow et al., 2009) and numerical ocean models (Hirschi et al., 2009).

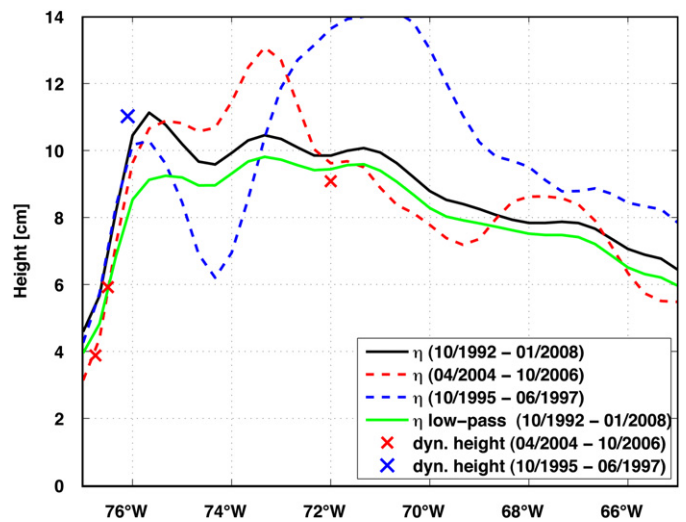


Fig. 8. RMS amplitude of sea surface height (η) along 26.5°N for the intervals October 1992–January 2008 (solid black line), April 2004–October 2006 (red dashed line) and October 1995–June 1997 (blue dashed line). Also shown is the amplitude of rms dynamic height fluctuations (dyn. cm; i.e. geopotential anomaly divided by the Earth's gravitational acceleration) at 200 m determined from the mooring density measurements at WB2, WB3 and WB5 (red crosses). The blue cross denotes dynamic height computed from density at mooring “C” of the ACCP-3 experiment (Johns et al., 2005). The green line shows the rms amplitude of η along 26.5°N for 2-year low-pass filtered data for the interval October 1992–January 2008. (For interpretation of the references to color in this figure legend, the reader is referred to the web version of this article.)

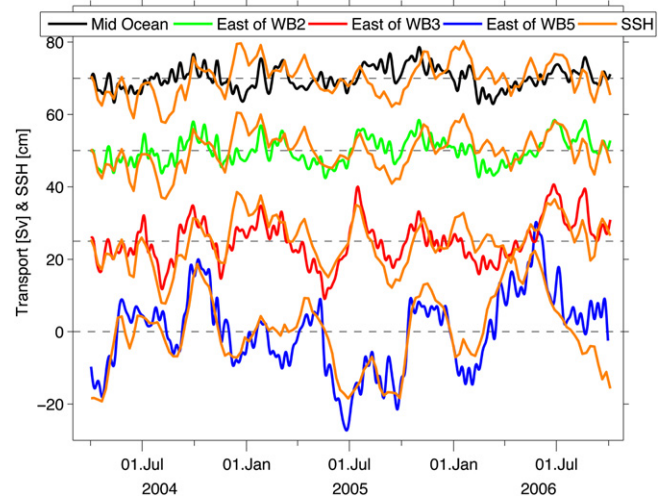


Fig. 9. Upper mid-ocean northward transport fluctuations in Sv shallower than 1000 m in black and eastward of moorings WB2 (green), WB3 (red) and WB5 (blue) to the eastern boundary off Morocco. Transports are offset by 25 Sv between each curve. Fluctuations of sea surface height in cm over the full mid-ocean section and to each mooring location are shown in orange. (For interpretation of the references to color in this figure legend, the reader is referred to the web version of this article.)

However, a high correlation is observed between SSH and the mid-ocean transport integrated from the African margin to the western moorings that are located offshore away from the western boundary (e.g. WB5) (Fig. 9). It seems that SSH is unlikely to be a useful predictor on subannual to interannual timescales of MOC variability at 26.5°N , but the mid-ocean variability offshore from the western boundary – the wind driven subtropical gyre – may be monitored by SSH variability.

The first 4 years of MOC observations at 26.5°N also suggest the presence of a seasonal cycle, which partly reflects the seasonal

cycle observed for the upper mid-ocean transport T_{UMO} . Recent work has shown that for T_{UMO} this seasonal variability has its origin at both the eastern and western margins. The slightly larger contribution originates from the eastern margin and can be explained by the heaving of isopycnals linked to the seasonal cycle of the wind-stress curl at the eastern margin (Kanzow et al., 2010; Chidichimo et al., 2010).

Bryden et al. (2009) show that at 4000 m depth at the western boundary off Abaco, bottom pressure fluctuations compensate instantaneously for baroclinic fluctuations in the strength and structure of the Deep Western Boundary Current. Therefore, baroclinic fluctuations in the Deep Western Boundary Current are compensated locally by bottom pressure fluctuations and so there is no mid-ocean flow resulting from fluctuations in the Deep Western Boundary Current. Residual bottom pressure fluctuations at the western boundary (bottom pressure fluctuations minus bottom pressure, which account for baroclinic variability of the Deep Western Boundary Current) compensate for fluctuations in Florida Current transport. Thus fluctuations in both the Florida Current and Deep Western Boundary Currents are compensated barotropically very close to the western boundary.

4. Discussion and summary

The 4 years of MOC observations have already provided an unprecedented insight into the MOC variability. With the initial measurements we were also able to determine that the historic estimates of the strength of the MOC, based on synoptic ship-board expeditions (Bryden et al., 2005), were within the range of subannual variability of the MOC (Cunningham et al., 2007).

One aspect that needs to be better understood and which is the subject of ongoing research is the climatic relevance of the MOC observations. A question of particular interest is whether we can use the RAPID data to improve climate predictions (on seasonal to perhaps decadal timescales). On the way to address this question we will need to be able to put the local MOC observations from 26.5°N into a wider spatial context and try to establish the meridional coherence of the observed MOC variability. Does the meridional coherence depend on the frequency (i.e. are subannual signals mainly local to 26.5°N while inter-annual and longer signals reflect processes affecting a large fraction of the North Atlantic basin (e.g. Bingham et al., 2007)?).

To address these points we will need to make use of observations from other locations and numerical models. Numerical studies suggest that fast propagating boundary waves can lead to meridionally coherent MOC changes. This was found for idealised model setups (e.g. Kawase, 1987, Johnson and Marshall, 2002) and in more realistic models (e.g. Bingham et al., 2007, Biastoch et al., 2008, Zhang, 2008). However, model results also suggest that locally, large high-frequency MOC variability could mask the coherence (e.g. Hirschi et al., 2007). To assess whether meridionally coherent MOC changes can be observed, the MOC transport from 26.5°N needs to be considered alongside data from other observing systems. From 2000 to 2009 the Meridional Overturning Variability Experiment (MOVE) provided NADW observations at 16°N in the Atlantic (e.g. Kanzow et al., 2006, 2008). Additionally, continuous observations have been made at the western boundary at 40°N since 2004 in the framework of the RAPID funded Western Atlantic Variability Experiment (WAVE, <http://www.pol.ac.uk/home/research/theme10/rapidII.php>, Hughes et al., 2002). Bottom pressure measurements are available at 26.5°N, as well as at the locations of MOVE and WAVE and can be used to test on what timescales we find coherent signals between the different observing systems. Model studies suggest a close link between bottom pressure and MOC fluctuations (e.g. Roussenov et al., 2008). It

would also be instructive if we could compare transports, e.g. of NADW at 26.5°N and 16°N, in terms of transports in isopycnal coordinates as this could allow us to infer water mass changes between different latitudes. However, since the transports at 26.5°N and 16°N are obtained from density observations at only a few longitudes (“end point method”), the full zonal density structure is not available, which means that a projection of transports onto density coordinates is not obvious.

One possible way to overcome the inability of ocean models to reproduce the observed ocean circulation and the inevitable gaps in observations is to assimilate the observed MOC and other observational ocean data into numerical models. There are different data assimilation schemes (e.g. Wunsch and Stammer, 1998, Köhl and Stammer, 2008, Smith and Haines, 2008, Balmaseda et al., 2007) that assimilate data from hydrographic sections, Argo floats or from satellites with the aim to produce ocean states that are as close as possible to the real ocean (“ocean analyses”). Apart from providing global, physically consistent ocean states that are useful for studying ocean processes (e.g. Köhl, 2005; Cabanes et al., 2008), the value of these ocean analyses lies in their potential use for improving climate predictions. Smith et al. (2007) showed that the assimilation of ocean observations into their decadal prediction system (DePreSys) improved the forecast quality in a set of 10-year hindcasts. Research done in the framework of RAPID-WATCH will establish the value of the RAPID-MOC data from 26.5°N, when it is used as an additional constraint in ocean models and forecasting systems like DePreSys (Smith et al., 2010; Baehr, 2010).

The RAPID-MOC monitoring system is funded by NERC, NOAA and NSF for a total of 10 years through to 2014 and should document the size and structure of the subannual to interannual variability in the Atlantic MOC. From a 10-year record, we can compare the interannual variations in the MOC with Atlantic sea surface temperature variations and with the North Atlantic Oscillation index and start to understand links between the Atlantic meridional overturning circulation and climate. The observational estimates of MOC variability will also serve as a new benchmark against which the variability in coupled climate models (which exhibit substantially different amplitude and structure in MOC interannual variability) can be compared and validated. With a 10-year record of MOC strength and structure and by considering ocean observations from other locations in the North Atlantic (e.g. in the framework of the EU funded Thermohaline Overturning—at Risk? (THOR) project), we can also start to assess whether there is a statistically significant trend in the strength of the MOC above the subannual and interannual variability and we can build the groundwork for predicting the course of Atlantic climate change over the next 50 years.

Appendix

Data availability

Data from the RAPID project are logged with the British Oceanographic Data Centre (BODC) on acquisition. Following the NERC data policy for RAPID-WATCH (http://www.bodc.ac.uk/projects/uk/rapid/data_policy/), data are made freely available from the BODC website (<http://www.bodc.ac.uk>). Timeseries of the overturning and component transports, along with gridded mooring data, are available from the project webpage (<http://www.noc.soton.ac.uk/rapidmoc>).

The Florida Current cable data are made freely available by the Atlantic Oceanographic and Meteorological Laboratory

(<http://www.aoml.noaa.gov/phod/floridacurrent/>) and are funded by the NOAA Office of Climate Observations.

The surface layer or Ekman contribution to the MOC is calculated from winds obtained by the QuickSCAT satellite scatterometer (SeaWinds on QuickSCAT. Mission, <http://winds.jpl.nasa.gov/missions/quickscat/index.cfm>).

References

- Baehr, J., Hirschi, J., Beismann, J.-O., Marotzke, J., 2004. Monitoring the meridional overturning circulation in the North Atlantic: a model-based array design study. *Journal of Marine Research* 62, 283–312.
- Baehr, J., 2010. Influence of the 26°N RAPID/MOCHA array and Florida Current cable observations on the ECCO-GODAE state estimate. *Journal of Physical Oceanography* 40, 865–879.
- Balmaseda, M., Smith, G., Haines, K., Anderson, D., Palmer, T., Vidard, A., 2007. Historical reconstruction of the Atlantic Meridional Overturning Circulation from the ECMWF operational ocean reanalysis. *Geophysical Research Letters* 34, L23615.
- Baringer, M.O., Larsen, J.C., 2001. Sixteen years of Florida Current transport at 27°N. *Geophysical Research Letters* 28, 3182–3197.
- Biaostoch, A., Böning, C.W., Lutjeharms, J.R.E., 2008. Agulhas leakage dynamics affects decadal variability in overturning circulation. *Nature* 456.
- Bingham, R.J., Hughes, C.W., Roussenov, V., Williams, R.G., 2007. Meridional coherence of the North Atlantic meridional overturning circulation. *Geophysical Research Letters* 2007 (34), L23606.
- Broecker, W.S., Denton, G.H., 1989. The role of ocean-atmosphere reorganisations in glacial cycles. *Geochimica et Cosmochimica Acta* 53, 2465–2501.
- Bryden, H.L., Imawaki, S., 2001. Ocean heat transport. In: Siedler, G., Church, J., Gould, J. (Eds.), *Ocean Circulation and Climate*. Academic Press, pp. 455–474.
- Bryden, H.L., Longworth, H.L., Cunningham, S.A., 2005. Slowing of the Atlantic Meridional Overturning Circulation at 25°N. *Nature* 438, 655–657.
- Bryden, H.L., Mujahid, A., Cunningham, S.A., Kanzow, T., 2009. Adjustment of the basin-scale circulation at 26°N to variations in Gulf Stream, Deep Western Boundary Current and Ekman transports as observed by the RAPID array. *Ocean Science* 5, 421–433.
- Cabanes, C., Lee, T., Fu, L.-T., 2008. Mechanisms of interannual variations of the meridional overturning circulation of the North Atlantic Ocean. *Journal of Physical Oceanography* 38, 467–480.
- Chidichimo, M.P., Kanzow, T., Cunningham, S.A., Marotzke, J., 2010. The contribution of eastern-boundary density variations to the Atlantic meridional overturning circulation at 26.5°N. *Ocean Science* 6, 475–490.
- Cubasch, U., Meehl, G.A., Boer, G.J., Stouffer, R.J., Dix, M., Noda, A., Senior, C.A., Raper, S., Yap, K.S., 2001. Projections of future climate change, Chapter 9. In: Houghton, J.T. (Ed.), *Climate Change 2001: The Scientific Basis*. Cambridge University Press, pp. 525–582.
- Cunningham, S.A., Kanzow, T.O., Rayner, D., Baringer, M.O., Johns, W.E., Marotzke, J., Longworth, H.R., Grant, E.M., Hirschi, J.J.-M., Beal, L.M., Meinen, C.S., Bryden, H.L., 2007. Temporal variability of the Atlantic Meridional Overturning Circulation at 26.5°N. *Science* 317, 935–938.
- Cunningham, S.A., 2005a. RRS Discovery Cruises 277 (26 Mar.–16 Apr. 2004) and 278 (19 Mar.–30 Mar. 2004): monitoring the Atlantic Meridional Overturning Circulation at 26.5°N. *Cruise Report No. 53*, 103pp.
- Cunningham, S.A., 2005b. RRS Discovery Cruise 279, 04 Apr.–10 May 2004: a transatlantic hydrographic section at 24.5°N. *Cruise Report No. 54*, 198pp.
- Cunningham, S.A., Marsh, R., 2010. Observing and modeling changes in the Atlantic MOC. *Wiley Interdisciplinary Reviews: Climate Change* 1, 180–191.
- Curry, R., Dickson, B., Yashayaev, I., 2003. A change in the freshwater balance of the Atlantic Ocean over the past four decades. *Nature* 426, 826–829.
- Dansgaard, W., Johnsen, S.J., Clausen, H.B., Dahl-Jensen, D., Gundestrup, N.S., Hammer, C.U., Hvidberg, C.S., Steffensen, J.P., Sveinbjörnsdóttir, A.E., Jouzel, J., Bond, G., 1993. Evidence for general instability of past climate from a 250 kyr ice-core record. *Nature* 364, 218–220.
- Delworth, T.L., Mann, M.E., 2000. Observed and simulated multidecadal variability in the Northern Hemisphere. *Climate Dynamics* 16, 661–676.
- Dickson, R., Yashayaev, I., Meincke, J., Turrell, B., Dye, S., Holfort, J., 2002. Rapid freshening of the deep North Atlantic Ocean over the past four decades. *Nature* 416, 832–837.
- Ganachaud, A., Wunsch, C., 2002. Large-scale ocean heat and freshwater transports during the World Ocean Circulation Experiment. *Journal of Climate* 16, 696–705.
- Graf, J., Sasaki, C., Winn, C., Liu, T., Tsai, W., Freilich, M., Long, D., 1998. NASA scatterometer experiment. *Acta Astronautica* 43, 397–407.
- Gregory, J.M., Dixon, K.W., Stouffer, R.J., Weaver, A.J., Driesschaert, E., Eby, M., Fichefet, T., Hasumi, H., Hu, A., Jungclaus, J.H., Kamenkovich, I.V., Levermann, A., Montoya, M., Murakami, S., Nawrath, S., Oka, A., Sokolov, A.P., Thorpe, R.B., 2005. A model intercomparison of changes in the Atlantic thermohaline circulation in response to increasing atmospheric CO₂ concentration. *Geophysical Research Letters* 32, L12703. doi:10.1029/2005GL023209.
- Häkkinen, S., Rhines, P.B., 2004. Decline of subpolar North Atlantic circulation during the 1990s. *Science* 304, 555–559.
- Häkkinen, S., Rhines, P.B., 2009. Shifting Surface Currents in the Northern North Atlantic Ocean. *Journal of Geophysical Research* 114, C04005. doi:10.1029/2008JC004883.
- Hansen, B., Turrell, W.R., Østerhus, S., 2001. Decreasing outflow from the Nordic seas into the Atlantic Ocean through the Faroe Bank Channel since 1950. *Nature* 411, 927–930.
- Hátún, H., Sandø, A.B., Drange, H., Hansen, B., Valdimarsson, H., 2005. Influence of the Atlantic Subpolar Gyre on the thermohaline circulation. *Science* 309, 1841–1844.
- Hirschi, J., Marotzke, J., 2007. Reconstructing the meridional overturning circulation from boundary densities and the zonal wind stress. *Journal of Physical Oceanography* 37, 743–763.
- Hirschi, J., Baehr, J., Marotzke, J., Stark, J., Cunningham, S.A., Beismann, J.-O., 2003. A monitoring design for the Atlantic meridional overturning circulation. *Geophysical Research Letters* 30. doi:10.1029/2002GL016776.
- Hirschi, J.J.-M., Killworth, P.D., Blundell, J.R., 2007. Subannual, seasonal and interannual variability of the North Atlantic Meridional Overturning Circulation. *Journal of Physical Oceanography* 37, 1246–1265.
- Hirschi, J.J.-M., Killworth, P.D., Blundell, J.R., Cromwell, D., 2009. Sea Surface height signals as indicators for oceanic meridional mass transports. *Journal of Physical Oceanography* 39, 581–601. doi:10.1175/2008JPO3923.1.
- Holliday, N.P., Hughes, S.L., Bacon, S., Beszczynska-Möller, A., Hansen, B., Lavin, A., Loeng, H., Mork, K.A., Østerhus, S., Sherwin, T., Walczowski, W., 2008. Reversal of the 1960s to 1990s freshening trend in the northeast North Atlantic and Nordic Seas. *Geophysical Research Letters* 35, L03614. doi:10.1029/2007GL032675.
- Huber, C., Leuenberger, M., Spahni, R., Flückiger, J., Schwander, J., Stocker, T.F., Johnson, S., Landais, A., Jouzel, J., 2006. Isotope calibrated Greenland temperature record over Marine Isotope Stage 3 and its relation to CH₄. *Earth and Planetary Science Letters* 243, 504–519. doi:10.1016/j.epsl.2006.01.002.
- Hughes, C., D. Marshall and R. Williams. 2002. A monitoring array along the western margin of the North Atlantic, Research Proposal submitted to Natural Environment Research Council.
- IPCC, 2007. Summary for policymakers. In: Solomon, S., Qin, D., Manning, M., Chen, Z., Marquis, M., Averyt, K.B., Tignor, M., Miller, H.L. (Eds.), *Climate Change 2007: The Scientific Basis*. Contribution of Working Group I to the Fourth Assessment Report of the Intergovernmental Panel on Climate Change. Cambridge University Press, Cambridge, New York.
- Johns, W.E., Kanzow, T., Zantopp, R., 2005. Estimating ocean transports with dynamic height moorings: an application in the Atlantic Deep Western Boundary Current at 26°N. *Deep-Sea Research I* 52, 1542–1567.
- Johns, W.E., Beal, L.M., Baringer, M.O., Molina, J., Rayner, D., Cunningham, S.A., Kanzow, T.O., 2007. Variability of shallow and Deep Western Boundary Currents off the Bahamas during 2004–2005: results from the 26°N RAPID-MOC array. 2008. *Journal of Physical Oceanography* 38, 605–623.
- Johnson, H.L., Marshall, D.P., 2002. A theory for the surface Atlantic response to thermohaline variability 32, 1121–1132.
- Kanzow, T., Send, U., Zenk, W., Chave, A.D., Rhein, M., 2006. Monitoring the integrated deep meridional flow in the tropical North Atlantic: long-term performance of a geostrophic array. *Deep Sea Research I* 53, 528–546.
- Kanzow, T., Cunningham, S.A., Rayner, D., Hirschi, J.J.-M., Johns, W.E., Baringer, M.O., Bryden, H.L., Beal, L.M., Meinen, C.S., Marotzke, J., 2007. Observed flow compensation associated with the MOC at 26.5°N in the Atlantic. *Science* 317, 938–941.
- Kanzow, T., Send, U., McCartney, M., 2008. On the variability of the deep meridional transports in the tropical North Atlantic. *Deep-Sea Research I* 55, 1601–1623.
- Kanzow, T., Johnson, H., Marshall, D., Cunningham, S.A., Hirschi, J.J.-M., Mujahid, A., Bryden, H.L., Johns, W.E., 2009. Basin-wide integrated volume transports in an eddy-filled ocean. *Journal of Physical Oceanography* 39, 3091–3110.
- Kanzow, T., Cunningham, S.A., Johns, W.E., Hirschi, J.J.-M., Marotzke, J., Baringer, M.O., Meinen, C.S., Chidichimo, M.P., Atkinson, C., Beal, L.M., Bryden, H.L., Collins, J., 2010. Seasonal variability of the Atlantic meridional overturning circulation at 26.5°N. *Journal of Climate* 23, 5678–5698.
- Kawase, M., 1987. Establishment of deep ocean circulation driven by deep-water production. *Journal of Physical Oceanography* 17, 2294–2317.
- Knight, J.R., Allan, R.J., Folland, C.K., Vellinga, M., Mann, M.E., 2005. A signature of persistent natural thermohaline circulation cycles in observed climate. *Geophysical Research Letters* 32, L20708. doi:10.1029/2005GL024233.
- Köhl, A., 2005. Anomalies of Meridional Overturning: mechanisms in the North Atlantic. *Journal of Physical Oceanography* 35, 1455–1472.
- Köhl, A., Stammer, D., 2008. Variability of the Meridional Overturning in the North Atlantic from the 50-year GECCO State estimation. *Journal of Physical Oceanography* 38, 1913–1930.
- Larsen, J.C., 1992. Transport and heat flux of the Florida Current at 27°N derived from cross-stream voltages and profiling data: theory and observations. *Philosophical Transactions of the Royal Society of London A* 338, 169–236.
- Lherminier, P., H. Mercier, C. Gourcuff, Treguier, A.M., 2006. MOC observations between Greenland and Portugal in Summers 1997, 2002 and 2004. EGU Abstract, presented in Vienna in April.
- Marotzke, J., Cunningham, S.A., Bryden, H.L., 2002. Monitoring the Atlantic meridional overturning circulation at 26.5°N, Research Proposal submitted to Natural Environment Research Council.
- Olsen, S.M., Hansen, B., Quadfasel, D., Østerhus, S., 2008. Observed and modelled stability of overflow across the Greenland-Scotland ridge. *Nature* 455, 519–522. doi:10.1038/nature07302.
- Østerhus, S., Gammelsrod, T., 1999. The abyss of the Nordic Seas is warming. *Journal of Climate* 12, 3297–3304.
- Roussenov, V.M., Williams, R.G., Hughes, C.W., Bingham, R., 2008. Boundary wave communication of bottom pressure and overturning changes for the North

- Atlantic. *Journal of Geophysical Research* 113, C08042. doi:10.1029/2007/JC004501.
- Smeed, D.A. et al., 2010. *Bellamite* and *Dynamite* RAPID Deployment Report, National Oceanography Centre, Southampton, Cruise Report No. 44.
- Smith, D.M., Cusack, S., Colman, A.W., Folland, C.K., Harris, G.R., Murphy, J.M., 2007. Improved surface temperature prediction for the coming decade from a global climate model. *Science* 317, 796–799.
- Smith, G.C., Haines, K., 2008. Evaluation of the S(T) assimilation method with the argo dataset. *Quarterly Journal of the Royal Meteorological Society* 135, 739–756.
- Smith, G.C., Haines, K., Kanzow, T., Cunningham, S.A., 2010. Impact of hydrographic data assimilation on the modelled Atlantic meridional overturning circulation. *Ocean Science* 6, 761–774.
- Vellinga, M., Wood, R.A., 2002. Global climatic impacts of a collapse of the Atlantic thermohaline circulation. *Climatic Change* 54, 251–267.
- Visbeck, M., E.P. Chassignet, R. Curry, T. Delworth, Dickson, B., Krahnmann, G., 2003. The ocean's response to North Atlantic Oscillation variability. In: The North Atlantic Oscillation, J.W. Hurrell, Y. Kushnir, G. Ottersen, M. Visbeck (Eds.), *Geophysical Monograph Series*, vol. 134, pp. 113–146.
- Webb, D.J., 1996. An ocean model code for array processor computers. *Computers & Geosciences* 22, 569–578.
- Whitworth III, T., Peterson, R.G., 1985. Volume transport of the Antarctic Circumpolar Current from bottom pressure measurements. *Journal of Physical Oceanography* 15, 810–816.
- Wunsch, C., Stammer, D., 1998. Satellite altimetry, the marine geoid, and the oceanic general circulation. *Annual Review of Earth and Planetary Sciences* 26, 219–253.
- Zhang, 2008. Coherent surface-subsurface fingerprint of the Atlantic meridional overturning circulation. *Geophysical Research Letters* 35, L20705. doi:10.1029/2008GL035463.